

Resistivity Survey in the Alid Geothermal Area, Eritrea, a Joint Interpretation of TEM and MT Data

Hjálmar Eysteinsson, Andemariam Teklesenbet, Guðni Karl Rosenkjær and Ragna Karlisdóttir

ISOR, Iceland Geosurvey, Grensasvegur 9, 108 Reykjavík Iceland.

he@isor.is

Keywords: Resistivity, MT, TEM, Alid, Eritrea
Geothermal, joint inversion

ABSTRACT

A geophysical survey of the Mt. Alid geothermal area in Eritrea was performed in late 2008. The aim of the survey was to delineate the geothermal reservoir by the use of Transient Electro Magnetism (TEM) and Magnetotelluric (MT) resistivity soundings. The original plan was to cover the area of Mt. Alid and its nearest vicinity. The terrain, however, was very difficult for vehicles and bikes used for transportation of the equipment and inaccessible at times. The area to the west and southwest of the mountain was covered as well as the top of Mt. Alid, within the allotted timeframe. A total of 67 TEM and 52 MT soundings were performed in 24 days. The TEM and MT soundings were performed in the same place. The TEM revealed the shallow resistivity structure and MT the deeper part. The TEM data were also used for static shift correction in the MT data through a joined 1-D inversion of the two data sets.

A SW-NE lineament is detected at a depth interval of 500 metres to 2 km, and interpreted as a transform fault intersecting the geothermal reservoir which most likely controls the main upflow from the reservoir.

The surface on the southwest flanks of Mt. Alid has an area with exceptional vegetation in comparison to the barren dry volcanic landscape around. This indicates moisture and water in the ground that could be explained by steam flowing up from the geothermal reservoir.

1. INTRODUCTION

In November 2008 ISOR (Iceland Geosurvey) and the GSE (Geological survey of Eritrea) conducted a geophysical survey in the Alid geothermal system in Eritrea, financed by the Icelandic Developing Agency (ICEDA). The Alid volcanic centre is located along the axis of the Danakil depression, a graben trace of a crustal spreading centre that radiates NNW from a plate-tectonic triple junction situated within a complexly rifted, and faulted basaltic lowland called the Afar triangle (Figure 1). The Danakil depression is a subaerial segment of the spreading system that is opening to form the Red Sea. Crustal spreading along the axis of the Red Sea is transferred to spreading along the Danakil segment in a right stepping en echelon pattern, Barberi and Varet (1977). The northern Danakil depression lies near or below sea level for the most of its extent. It is surrounded by the Danakil horst to the east and the Eritrean plateau to the west

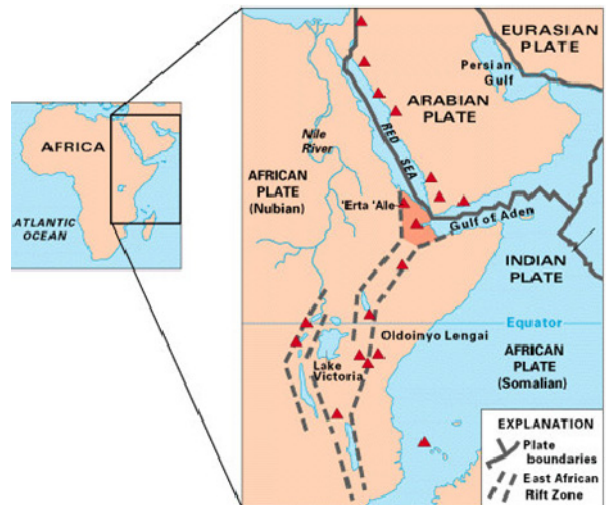


Figure 1: The east African rift system, showing some of the historically active volcanoes (red triangles) and the Afar Triangle (shaded, center) — a triple junction where three plates are pulling away from one another. Mt Alid is some 150 km NNW of the Eara Ale volcano in Ethiopia. (Figure from USGS)

Mt. Alid (Figure 2) rises up to about 700 metres above the flat plains of the Danakil depression, to a summit of 904m. The mountain is elongated with major axis of 7 km in an ENE-WSW direction, perpendicular to the graben, and a minor axis that is about 5 km long, parallel to the graben.

Geological and geochemical studies imply that a high temperature geothermal system underlies the Alid volcanic centre. Fumaroles and boiling pools mainly on the northern part of Mt. Alid suggest that an active hydrothermal system underlies that part of the mountain. Geothermometers indicate temperatures exceeding 250 °C in the reservoir, Lowenstern et al. (1999); Clyne et al., (2005).



Figure 2: Mount Alid seen from SSW.

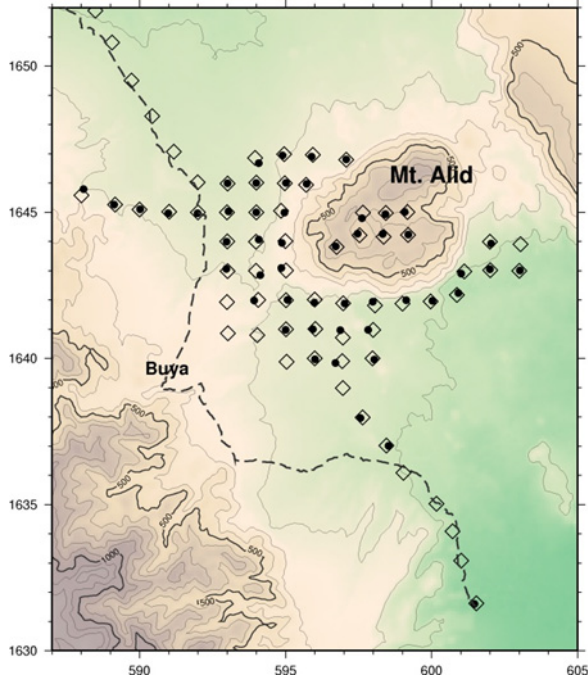


Figure 3: Location of TEM (open diamonds) and MT (filled points) soundings. The road is shown by black dashed line. Contours are elevation in meters. Coordinates are UTM km units

2. FIELD SURVEY

A camp was set up in the small village Boya a few km SW of Mt Alid (Figure 3). The survey lasted from 21/11 to 14/12 2008. During that time 67 TEM central loop soundings where performed and 52 MT sites. Four, six-wheel bikes were used to travel around the area with the equipment, two bikes for each group. The locations of soundings are shown on Figure 3. Originally the plan was to measure MT and TEM on top of Mt Alid and in its' surroundings. However, due to rough and inaccessible lava-flows both SW and NE of Mt. Alid, we were only able to access the area to the west and south-west of the mountain. Camels were used to carry the equipment on top of Mt. Alid.

In the TEM soundings electrical current is transmitted into a big loop of wire ($300 \times 300 \text{ m}^2$) laid on the ground. This current produces a magnetic field. The current is abruptly turned off and the decaying magnetic field causes induction currents in the ground. The strength of the induced currents is dependent on the resistivity structure below the survey site. The ground response is measured by a small coil in the centre of the big transmitting loop. The time decaying signal is measured from $88 \mu\text{s}$ to 70 ms from the time of turning of the current. The TEM exploration depth for the conductive environment in the Alid area is usually less than 500 m.

In the MT method, the natural fluctuations of the earth's magnetic field are used as signal source. Those fluctuations induce currents in the ground and are measured on the surface with two horizontal and orthogonal electrical dipoles and the magnetic field is measured in three orthogonal directions. The instrument were run for about 20 hours (or one day), for each MT sounding. However, due to bad or low signal strength we often had to keep the sites running for more than one day. The period range of the MT soundings is from 0.003 seconds (320 Hz) and up to about 1000 seconds. This yields an exploration depth down to about 10 km for the conductive environment in the Alid

area.

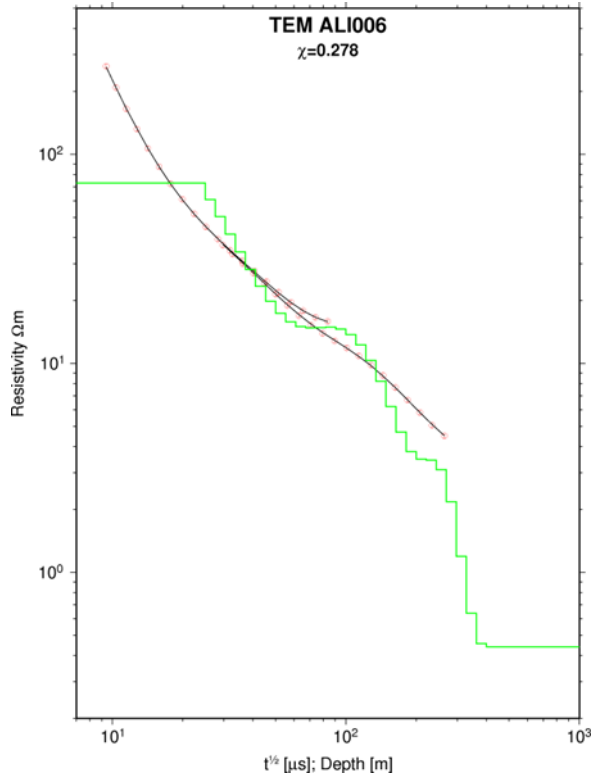


Figure 4: Apparent resistivity (red dots) of TEM sounding ALI006 as a function of square root of time from current turnoff. The black curve is the model response of the model shown by green lines (Occam inversion result)

3. DATA PROCESSING AND INTERPRETATION

An example of TEM data is given in Figure 4 showing the apparent resistivity as a function of the square root of time in μs , from the current turn off. The data quality is extremely good due to very low resistivity in the area. An Occam inversion of this data yields the model shown by the green lines on the figure, Constable et.al (1987), deGroot-Hedlin and Constable (1990). A low resistivity of about $0.3 \Omega\text{m}$ is located at about 300 m depth. In this extremely conductive environment the depth of penetration of the TEM signal is only about 300-400 meters. This low resistivity is about the same resistivity as in the conductive ocean, and could well reflect an old ocean bottom.

From the Fourier transform of the measured time series of the electrical and magnetic fields, the impedance (Z) is calculated which is dependent on the earth's resistivity structure. The impedance is found from the relationship between the two fields according to:

$$\begin{bmatrix} \mathbf{Ex} \\ \mathbf{Ey} \end{bmatrix} = \begin{bmatrix} Z_{xx} & Z_{xy} \\ Z_{yx} & Z_{yy} \end{bmatrix} \begin{bmatrix} \mathbf{Hx} \\ \mathbf{Hy} \end{bmatrix} \quad (1)$$

where \mathbf{Ex} and \mathbf{Ey} are horizontal orthogonal electric fields, \mathbf{Hx} and \mathbf{Hy} are orthogonal magnetic fields and Z_{ij} are the elements of the complex impedance tensor. Figure 5 shows the amplitude and phase of those elements as a function of period for MT site 006 located near the TEM site ALI006. The period is a kind of a depth scale since the longer the period is, the deeper the electromagnetic wave penetrates. For a 1-D model assumption the diagonal elements of the impedance tensor should be small, i.e. $Z_{xx}=Z_{yy}=0$; and for a 2-D model it is possible to rotate the coordinate system in such a manner that both the diagonal elements are zero.

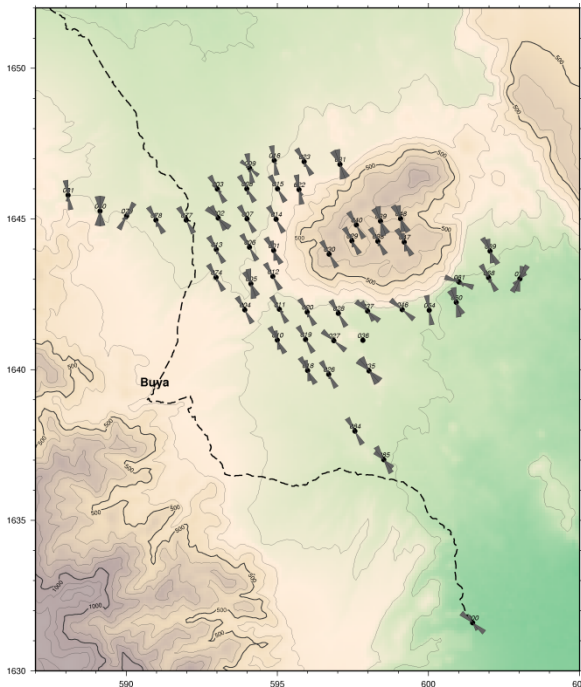


Figure 6: Rose diagram of electrical strike direction at periods greater than 10 seconds

Figure 5 shows that the diagonal elements of the impedance tensor are not zero, but they are more than an order of

magnitude lower than the off diagonal elements up to about 1 second, and the main impedance elements (Z_{xy} and Z_{yx}) are about the same indicating approximately a 1-D resistivity structure for the shallow part. At greater depths, i.e. for periods greater than 10 seconds, all the impedance elements are in the same order of magnitude showing a high degree of three-dimensionality in the resistivity structures below this site. This is true for many of the MT sites in the Alid area.

The rotation that minimizes the diagonal elements of the impedance tensor (or maximizes the off diagonal elements), is named the electrical strike direction. This direction can be calculated for each period and for a clear electrical strike and good data quality they would all yield the same direction. A rose diagram of the electrical strike, for periods greater than 10 seconds is shown on Figure 6 and clearly shows that the general strike is about N30W for most of the sites. This means that deeper electrical structures are parallel to the graben. Shorter periods, (i.e. shallower structures) do show more variability in the strike direction.

It is evident that the MT data deviate strongly from 1-D model responses at periods greater than 1 second and a 3-D inversion is required to fully explain the MT data. However, 3-D MT inversion is very time consuming and is beyond the scope of this work. Therefore we apply 1-D inversion of the MT data as a starting point for the complex resistivity structure in the Alid area. We could invert for either xy or the yx apparent resistivity and phase

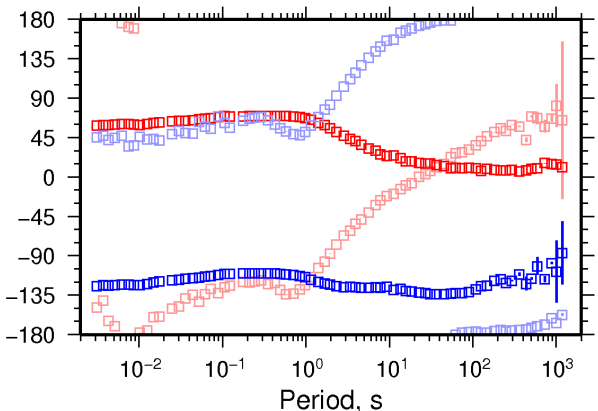
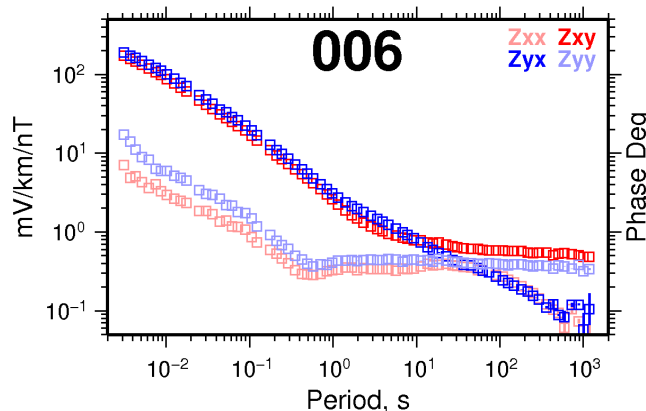


Figure 5: Amplitude and phase of the impedance elements from MT site 006, as a function of period

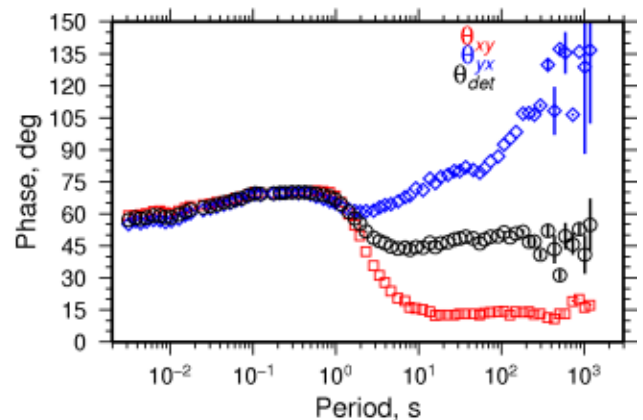
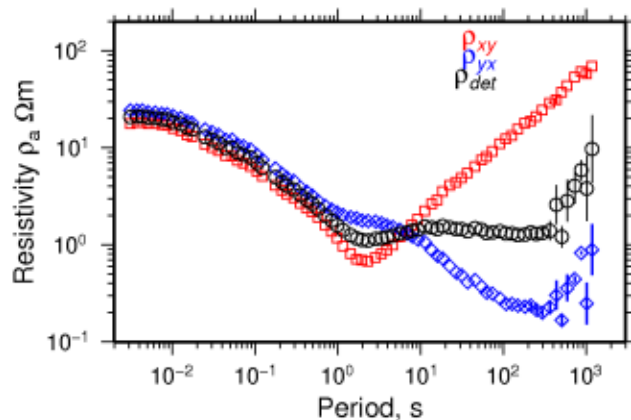


Figure 7: Apparent resistivity and phase for MT site 006, calculated from Z_{xy} , Z_{yx} and Z_{det}

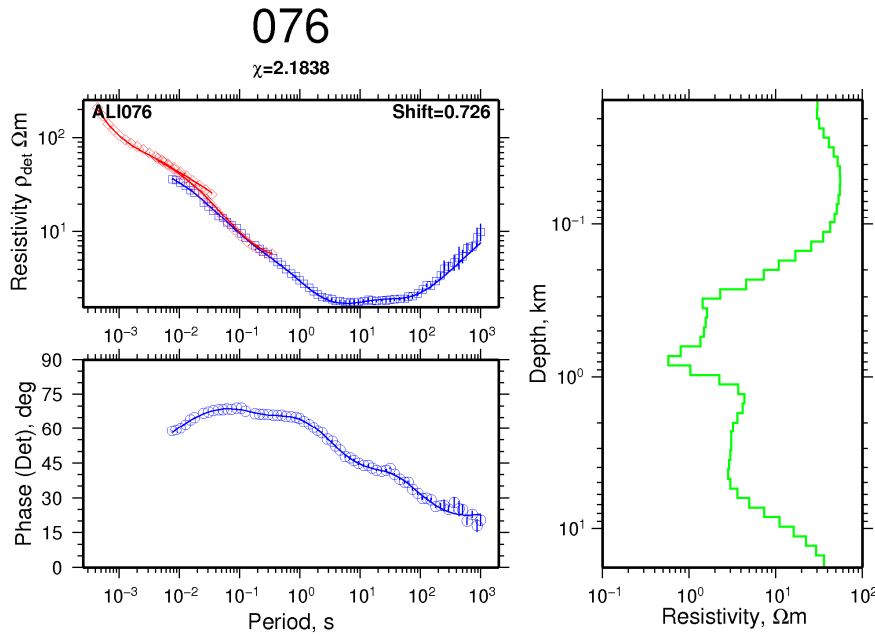


Figure 8: Inversion results of data from MT station 076 (blue points) and TEM station ALI076 (red points). The best fitting telluric shift value is 0.726. The response of the model to the right is shown by a red (TEM) and blue (MT) curves

parameters, but we prefer to invert for rotationally invariant parameters such as the determinant-, effective- or geometric mean impedance. Based on comparison of model responses for 2- and 3-D models several authors have suggested that the determinant impedance is the most appropriate for 1-D inversion, Park and Livelybrook (1989); Rangabayaki (1984); Ingham (1988). Therefore we prefer to use the determinant impedance for our 1-D inversion, defined as

$$Z_{det} = \sqrt{Z_{xx}Z_{yy} - Z_{xy}Z_{yx}} \quad (2)$$

A plot of the apparent resistivity and phase for MT site 006 is shown in Figure 7, both xy and yx values (in preferred rotation, -25°) as well as the invariant determinant

4 TELLURIC SHIFT IN MT SOUNDINGS

The MT method, like all resistivity methods where the electric field is measured on the surface, suffers from a problem called the telluric shift or static shift problem, e.g. Park et.al. (1983), Wannamaker et.al. (1984), Park (1985). The reason for this is local resistivity inhomogeneity which distorts the electric field, independent of period. The result of this is that the apparent resistivity values have an unknown multiplier (shift of logarithmic value). The TEM soundings do not suffer this problem because they measure magnetic induction in a receiver coil. By interpreting TEM and MT soundings made at the same (or nearly the same) location together, the TEM data can be used to determine the unknown multiplier of the MT apparent resistivity e.g. Sternberg et.al. (1988).

This is why the TEM soundings are essential in areas where telluric shifts in MT soundings can be expected, such as in the Mt. Alid volcanic area. This is the reason for setting up the TEM sites in the same location, or close to the location of an MT site. The maximum distance between an MT site and a corresponding TEM site is 260 m.

The shift parameter is found through a joint inversion of the TEM and the MT data where the shift value for the MT-apparent resistivity data is one of the inversion parameters. An example of an inversion result is shown in Figure 8. The MT data points are shown by blue dots (apparent resistivity and phase) and the TEM data are shown by red apparent

resistivity points. The 1-D model is shown to the right and its TEM and MT response is shown by red and blue curves respectively. The model response fits the data quite well. The TEM data on Figure 8 has been changed from time to period according to the method described by Sternberg et.al. (1988).

The distribution of all the shift parameters in the MT soundings is shown in Figure 9. If the telluric shift in the MT data is random, one would expect a mean value of 1, but as is shown in Figure 9, the mean value is about 0.7, with minimum and maximum values of 0.1 and 1.7 respectively. A shift factor of 0.1 means that the apparent resistivity data have been shifted down by an order of magnitude due to local resistivity inhomogeneities. Uncorrected interpretation of that sounding would have yielded a model having the resistivity about one order of magnitude lower, where the depths of the layers were about 3 times shallower. A mean shift less than one is quite common in a volcanic environment. In MT studies in Iceland where TEM has been used for static shift correction, similar mean shift are found, around 0.8, e.g. Árnason et.al. (2009).

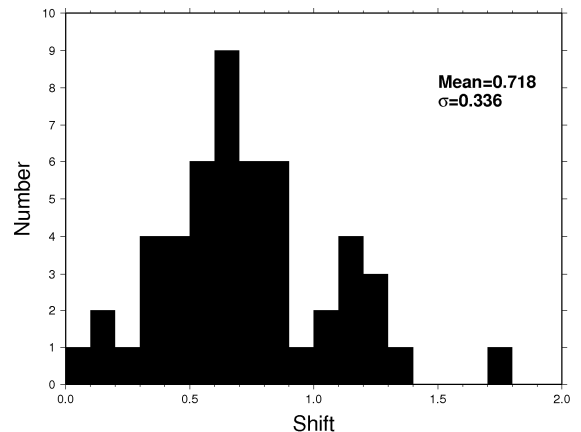


Figure 9: Histogram of shift factors applied to the MT apparent resistivity curves

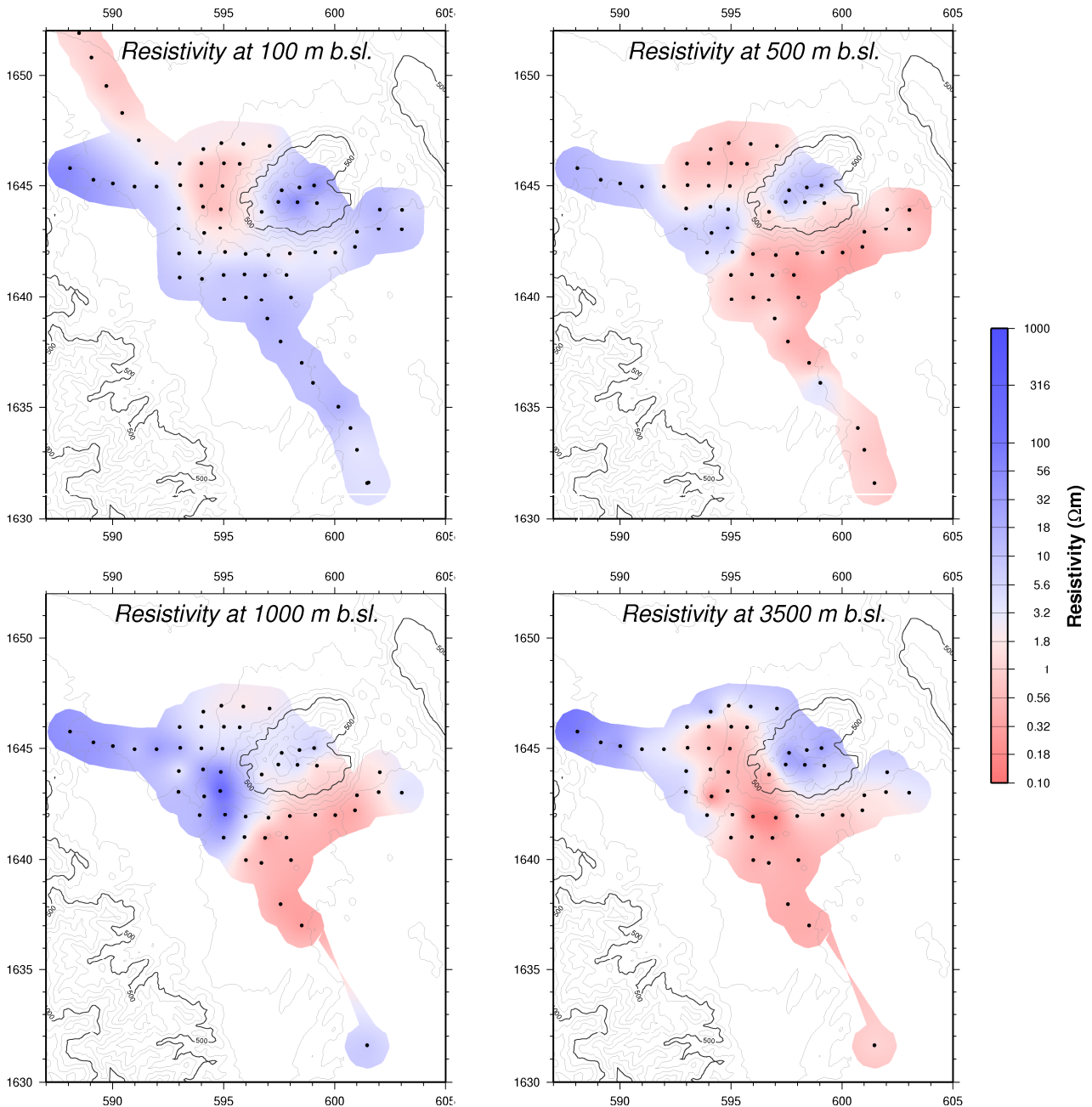


Figure 10: Resistivity at 100, 500, 1000, and 3500 m below sea level

5 RESULT OF JOINT INVERSION OF MT AND TEM DATA

The 1-D TEM/MT joint inversion results are compiled into a 3-D resistivity structure and are presented by iso-resistivity maps at various elevations above and below the sea level, and by resistivity cross sections through the survey area.

For each site a depth of exploration is estimated. At sites where only TEM sounding is present the depth of exploration is usually no more than about 500 meters. For MT sites where data quality is bad at long periods the depth of exploration is as low as 2 km, but generally 6–10 km. In some instances, where 3-D signal is strong in the long period MT data, a 1-D model could not be generated that fits both the apparent resistivity and phase, therefore the depth of penetration at those soundings is dramatically reduced for 1-D modelling. Thus, in generating the following figures (resistivity maps and cross sections), no resistivity information from a site is used at depths greater than the corresponding exploration depth.

Resistivity maps at 100, 500, 1000 and 3500 metres below sea level (m.b.s.l.) are shown on Figure 10. The topographic elevation is generally 100–200 metres above the sea level. At 100 m.b.s.l. a 1 Ωm low resistivity appears NW of Mt. Alid, which expands at deeper levels but is not observed below Mt. Alid. At 500 m.b.s.l. a high resistivity body appears to cut Mt. Alid in a WWS-NEE direction perpendicular to the rift system. At 1000 m.b.s.l. the low resistivity west and north of Mt. Alid has disappeared and a clear SW-NE resistivity boundary is observed under the southern part of the mountain. This boundary extends down to about 2000 metres.b.s.l. Below that level, a low resistivity appears again to the northwest of the mountain and is connected to the general low resistivity located to the south and southwest of the mountain where it continues to deeper levels. Again no low resistivity is seen below the mountain.

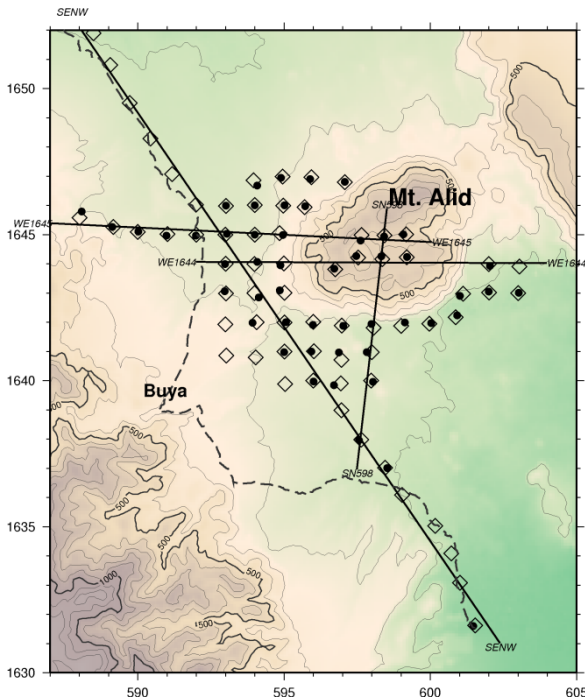


Figure 11: Location of resistivity cross sections in Figures 12-15

At 3500 m b.s.l. a clear low resistivity body with NNW-SSE direction is situated west of the mountain and connected to the broader low resistivity to the south. Note that at this depth the resistivity is lowest at the base of the Mt. Alid slopes, SW of it, where the resistivity gets as low as 0.3 Ω m. There appears to be a sharp resistivity boundary in NNW-SSE direction under the western part of the mountain that extends as deep as the resolution of the soundings. The resistivity cross sections display a better view about this boundary.

Below 3500 m b.s.l. a more general resistivity structure is observed. The low resistivity body west of the mountain

widens, and a clear low resistivity region is observed at the base of the mountain southwest of it. Figure 11 shows location of few resistivity cross sections through the area, shown on Figures 12-15. No resistivity values are shown below the estimated depth of resolution for each sounding.

A 25 km long SE-NW resistivity cross section is shown in Figure 12. Its location is west of Mt. Alid. All soundings with the name starting with ALI show the results from the TEM measurements only and therefore they have shallow penetration depth. The data clearly show a conductive shallow layer through the whole area at a few hundred metres depth. The sharp vertical resistivity boundary between sites 018 and 010, at the depth of 1–2 km b.s.l., is clear. South of this boundary the shallow low resistive layer adjoins to the deeper low resistivity body, seen at 1.5–2.5 km b.s.l. The fact that this deeper low resistivity body is seen in the southern most sounding, approximately 10 km away from the mountain, suggests that it exists over a very large area. However, its resistivity is somewhat higher there, than in the vicinity of Mt. Alid.

Figure 13 shows a south to north cross section through Mt. Alid. It clearly shows the SW-NE vertical resistivity boundary through the southern part of the mountain. Unfortunately MT sounding 036 does only have reliable data up to a few seconds, and therefore its exploration depth is shallow. South of that boundary the graben is very well conducting all the way down to the exploration depth of about 10 km. It must be emphasized that two and three dimensional effects are seen in the data at long periods, and thus 1-D model may not be reflecting the true resistivity at great depths. Only 3-D modelling could explain the data fully and therefore the true resistivity of the deeper structure.

Figures 14 and 15 show a west to east cross section through Mt. Alid. They clearly show the low resistivity body west of Mt. Alid at about 2500 m depth. There appears to be a very sharp vertical boundary running NS under the western part of the mountain. Relatively high resistivity is observed under Mt. Alid.

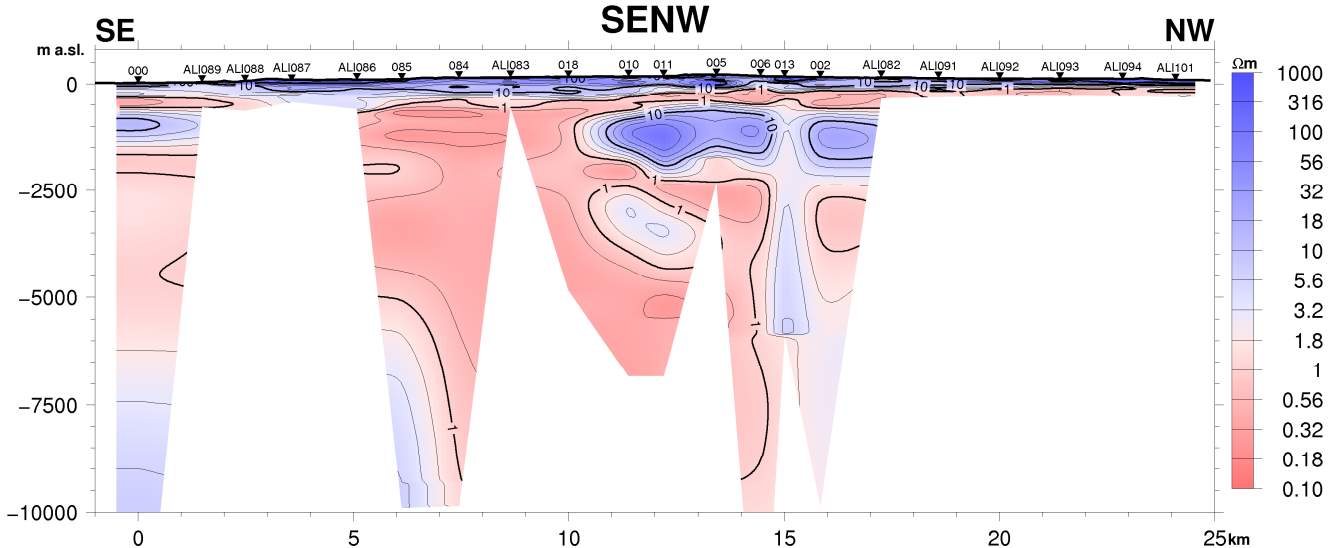


Figure 12: A resistivity cross section through the area, with NW-SE direction. The location of the section is shown on Figure 11

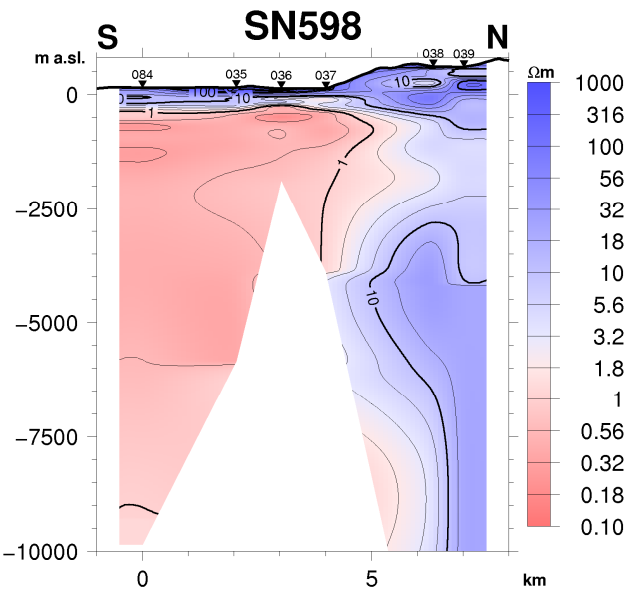


Figure 13: South to north resistivity cross section

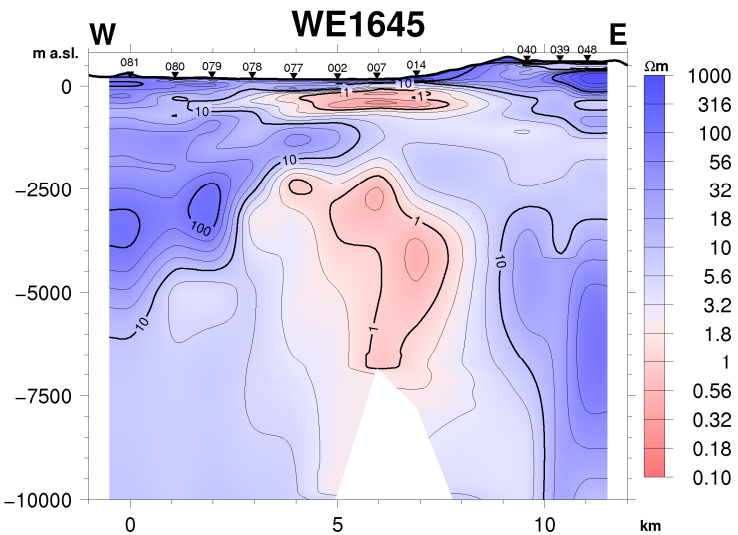


Figure 14: West to east resistivity cross section at Y coordinate location 1645

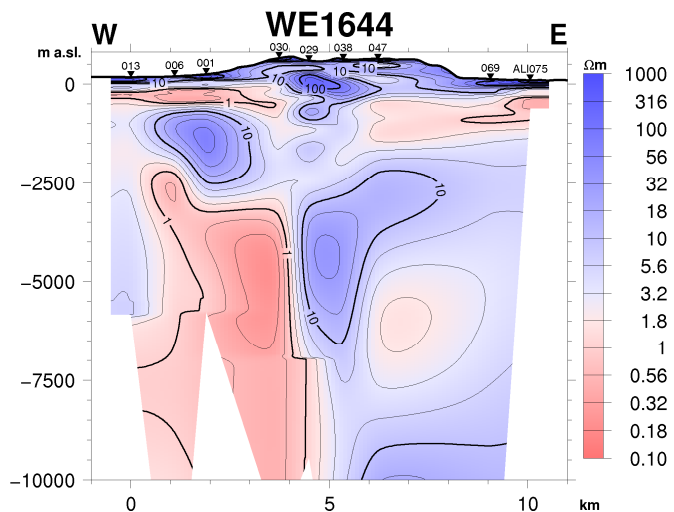


Figure 15: West to east resistivity cross section at Y coordinate location 1644

CONCLUSION

The resistivity structures of the Alid area have the following characters:

- **A thin low resistivity layer.** A shallow (at a few hundred metres depth) and thin (few hundred metres) low resistivity layer is seen in most of the soundings, except in those on the top of Mt. Alid.
- **A SW-NE lineament.** A conductive zone is seen down to about 6–7 km depth (and even more in some places) in the south and southwest of Mt. Alid. This zone has a sharp vertical boundary or a lineament in the depth interval from $\frac{1}{2}$ –2 km depth shown by a yellow line on Figure 16. This boundary is best seen on the iso-resistivity map at 1 km b.s.l. in Figure 10.
- **A low resistivity body.** Below the western part of Mt. Alid and to the west of the mountain there is a low resistivity body, approximately 3 km wide and with a NNW-SSE direction. It reaches the highest elevation at 2–3 km b.s.l., and extends down to a depth of about 7 km. The location of this body is shown on Figure 16, marked with a brown contour line.
- Beneath most of Mt. Alid there is rather **high resistivity**, compared to the surroundings, and no deep conductor, except in the western most sounding on the mountain.

The thin low resistivity layer seen down to 1000 metres depth is interpreted as the old conductive sea bed.

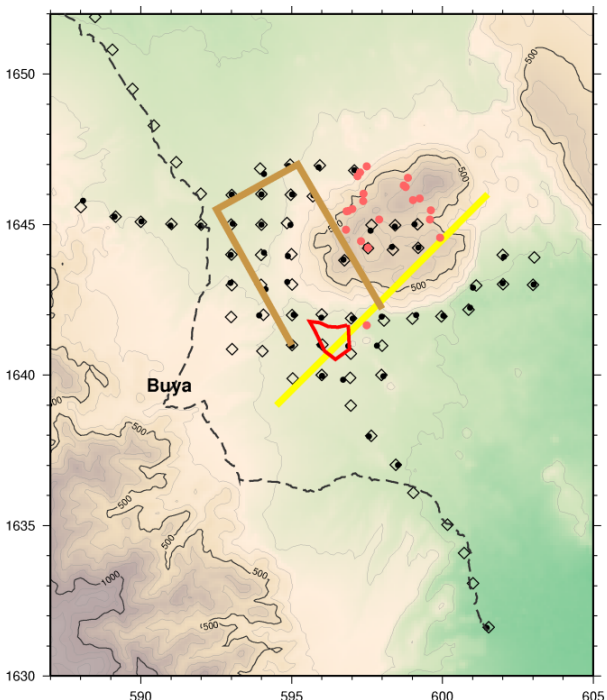


Figure 16: The Yellow line shows the location of the vertical resistivity boundary between $\frac{1}{2}$ and 2 km depth. The brown contour lines outline the low resistivity body west of Mt. Alid at about 2 km depth. Red dots are geothermal vents on Mt. Alid (data from Geological survey of Eritrea and one point found while surveying south of Alid), and the red polygon is the area of enhanced vegetation discussed in the text

According to Lowenstern et al. (1999), geological and geochemical studies imply that a high temperature geothermal system underlies the Alid volcanic centre. The resistivity survey does not cover enough area to compare

the resistivity structure beneath Mt. Alid to the structures all surrounding it. The high resistivity beneath Mt. Alid does not stand out as an anomaly, as it is not bounded to the east and north-east due to lack of soundings. Until we can determine whether the high resistivity represents a resistive body in low resistivity surroundings we cannot conclude that this high resistivity represents the geothermal heat source.

If this, however, were the case, i.e. the high resistivity under Mt. Alid represented the heat source, one would expect it to be surrounded by low resistivity bodies. From the results of this survey we see that the high resistivity has a very sharp SW-NE boundary with the low resistivity on the southern side. This boundary forms a clear lineament extending from the depth 500 m b.s.l. down to 2000 m b.s.l. From the depth of 3500 down as far as can be detected, there is a distinctive low resistivity body south-west of Mt. Alid. These low resistivity bodies to the south and west of the mountain could well be the part of a greater area surrounding Mt. Alid, but as of now, we do not have information on the resistivity to the east and northeast.

The lineament mentioned is sure to play a major role in the geothermal system. It most likely represents a SW-NE fault or a fault system that cuts under the southern part of the mountain. According to Clyne et al. (2005), some fumaroles on the top of the mountain, form weak $N45^\circ E$ alignments, the same direction as the lineament. The major axis of the mountain itself has this direction. A geological map in the paper of Clyne et al., show a shift in the fissure swarm through Mt Alid, where it intersects the NE-SW lineament. This could possibly indicate that the SW-NE lineament represents a transform fault underlying Mt. Alid.

At the SW slopes of Mt. Alid, an area, the size of about 1 km^2 , shows quite a different character in vegetation than the surrounding dry volcanic landscape. The growth of the vegetation is clearly influenced by water or moisture in the ground. It is reasonable to expect that this is due to steam, coming from the geothermal system below. This area is shown on Figure 16, marked by a red polygon. The area coincides with the NE-SW lineament, marked as a yellow line on the figure. This supports the idea that the transform fault or connected fault system takes part in or controls the upflow into the geothermal system.

With the information available on the resistivity structures, it is more difficult to explain the deep seated low resistivity body below the western part and west of Mt. Alid (brown contour lines on Figure 16). It is reasonable to assume that resistivity at such depths is influenced by high temperatures. It is also interesting to observe that the vegetated area is right above the top of the low resistivity body. However, this distinctive low resistivity body has to be seen in a greater context to be better understood. .

REFERENCES

Árnason, K., H. Eysteinsson, and G.P. Hersir. Joint 1D inversion of TEM and MT data and 3D inversion of MT data in the Hengill area SW Iceland. *Submitted to Geothermics* (2009),

Barberi F. and Varet Jacques.: Volcanism of Afar: Small-scale plate tectonic implications. *Geological Society of America Bulletin*, **88**. (1977), 1251-1266.

Clyne, M. A., Duffield, W. A., Fournier, R. O., Woldegiorgis, L., Janik, C. J., Kahsai, G., Lowenstern, J. B., Weldemariam, K., Smith, J. G. and Tesfai, T.

(2005). *Proceedings World Geothermal Congress (2005)*, Antalya, Turkey., 24.–29.

Constable, S. C., R. L. Parker, and C. G. Constable, Occam's inversion – A practical algorithm for generating smooth models from electromagnetic sounding data, *Geophysics*, 52 (03), (1987), 289–300.

deGroot-Hedlin, C., and S. Constable, Occam's inversion to generate smooth two-dimensional models from magnetotelluric data, *Geophysics*, 55 (12), (1990), 1613–1624.

Ingham, M. R. The use of invariant impedances in magnetotelluric interpretation. *Geophysical Journal*, 92, (1988), 165–169.

Lowenstern, J. B., Janik, C. J., Fournier, R. O., Tesfai, T., Duffield, W. A., Clyne, M. A., Smith, J. G., Woldegiorgis, L., Weldemariam, K. and Kahsai, G. (1999). A geochemical reconnaissance of the Alid volcanic center and the geothermal system, Danakil depression, Eritrea. *Geothermics*, (1999), 161–187.

Park, S.K., A.S. Orange, and T.R. Madden. Effects of three dimensional structure on magnetotelluric sounding curves: *Geophysics*, 48, (1983) 1402–1405.

Park, S.K. Distortion of magnetotelluric sounding curves by three dimensional structures, *Geophysics*, 50, (1985), 786–797.

Park, S. K. and Livelybrook, D. W.. Quantitative interpretation of rotationally invariant parameters in magnetotellurics. *Geophysics*, 54, (1989), 1483–1490.

Rangabayaki, R. P. An interpretive analyses of magnetotelluric data. *Geophysics* 49, (1984), 1730–1748.

Sternberg, B. K., Washburne, J. C. and Pellerin, L. Correction for the static shift in magnetotelluric, using transient electromagnetic soundings. *Geophysics*, 53, (1988), 1459–1468.

Wannamaker, P.E., Hohmann, G.W. and San Filipo, W.A. Magnetotelluric responses pf three dimensional bodies in layered earth. *Geophysics*, 49, (1984), 1517–1533.